JOURNAL OF COMPUTATIONAL PHYSICS **135,** 154–169 (1997)
ARTICLE NO. CP975699

A Numerical Method for the Study of the Circulation of the World Ocean

Kirk Bryan

Geophysical Fluid Dynamics Laboratory, ESSA, Princeton, New Jersey 08540

Received December 26, 1968

A model is presented for studying ocean circulation problems taking into account the complicated outline and bottom topography of the World Ocean. To obtain an efficient scheme for the study of low-frequency, large-scale current systems, surface gravity-inertial waves are filtered out by the ''rigid-lid'' approximation. To resolve special features of the ocean circulation, such as the Equatorial Undercurrent, the numerical model allows for a variable spacing in either the zonal or meridional direction. The model is designed to be as consistent as possible with the continuous equations with respect to energy. It is demonstrated that no fictitious energy generation or decay is associated with the nonlinear terms in the finite difference form of the momentum equations. The energy generation by buoyancy forces for the numerical model is also designed in such a way that no energy ''leak'' occurs in the transformation from potential to kinetic energy.

I. INTRODUCTION

Starting with the pioneering work of Ekman and gaining increasing momentum in the last two decades, considerable progress has been made in explaining some of the major features of the ocean circulation. An important gap has existed, however, between operational and theoretical studies. The fundamental problems in the dynamics of ocean currents which engaged the attention of theoretical oceanographers has often seemed quite remote from the task of interpreting the data on temperature, salinity, and other water mass properties brought back from oceanographic expeditions. Recent progress holds out some hope that this situation is changing. On the one hand, new techniques for making direct current measurements are producing a much more complete description of ocean currents, and of ocean turbulence on a smaller scale. On the other hand, more attention is being focused on those branches of hydrodynamics most closely related to ocean circulation studies. Renewed interest in carrying out laboratory experiments with rotating fluids has brought an appreciation of the importance of the basic work carried out by earlier investigators.

Reprinted from Volume 4, Number 3, October 1969, pages 347–376.

An impediment to progress in the theory of ocean circulation has been the mathematical difficulties of solving the equations of even very simplified ocean circulation models. This is caused by the complicated geometry of ocean basins, and more importantly by the nonlinear nature of the equations. The availability of large-scale computers in recent years has now made it possible to carry out ''numerical experiments'' using a direct computational approach in obtaining solutions to problems too complex to handle by any analytical method. The first ocean circulation research carried out along these lines was done in a series of studies by Sarkisyan [18, 19] in the Soviet Union.

The present paper describes in detail a computational procedure to be used in ocean circulation studies. While it has certain features in common to that used in two earlier studies of a baroclinic ocean [3, 4], the present method introduces many simplifications and is also generalized to handle an ocean basin with irregular coastlines and bottom topography. The principal difference in the present computational procedure and the method recently proposed by Crowley [5] involve the treatment of nonlinear terms, and the boundary condition of the vertical velocity at the ocean surface. The nonlinear terms in the present model are formulated on the basis of centered differencing using the same general method given by Fromm [7] and Arakawa [1]. Crowley uses a forward difference with respect to time and a ''time splitting'' procedure for evaluating the nonlinear advection similar to that proposed by Marchuk [13]. The present procedure has the advantage compared to the Marchuk method of exactly conserving certain energetic properties of the flow in the inviscid case. It has the drawback, however, of requiring the retention of two time-levels of the variables in the machine memory. A demonstration of the energetic properties of the method is given in the Appendix.

Crowley [5] allows vertical displacements of the ocean surface, while these displacements are not allowed in the present scheme. This constraint is called the ''rigid-lid'' approximation. The effect is to include pressure variations at the upper surface, but to exclude the kinematic effects of surface variations. External inertial-gravitational waves

0021-9991/97 $25.00

are filtered out with no distortion of the steady-state ocean circulation and very little distortion of low-frequency motions. Since external gravity waves move rapidly compared to other types of disturbances in the ocean, removing these high speed waves allows an order of magnitude increase in the time step. This enormous economy in calculation justifies the increased complexity in the numerical scheme required by the ''rigid-lid'' approximation.

II. EQUATIONS OF THE MODEL

General Forms of the Equations

In formulating the equations of the model the Navier–Stokes equations have been modified in three important respects. First, density differences are neglected except in the buoyancy term, i.e. the Boussinesq approximation. Second, the local acceleration and other terms of the same order have been neglected in the equation of motion for the w-component, reducing it to the hydrostatic approximation. The hydrostatic approximation may be shown to be highly accurate as long as the aspect ratio of bottom topography is much less than unity. Third, only the large-scale motion is treated explicitly, and the stresses exerted by smaller-scale motions are taken into account by a ''turbulent viscosity'' hypothesis. Ordinary viscosity and conductivity are very much smaller effects and are consequently neglected.

Let

$$\begin{aligned} m &= \sec\varphi \\ n &= \sin\varphi \\ u &= a\dot{\lambda}/m \\ v &= a\dot{\varphi}, \end{aligned} \tag{2.1}$$

where a is the radius of the earth, φ is latitude, and λ is longitude. It will be convenient to define an advection operator, such that

$$\mathscr{L}\mu = \frac{m}{a}\left[(u\mu)_\lambda + (v\mu/m)_\varphi\right] + (w\mu)_z \tag{2.2}$$

where μ is some scalar quantity. The equations of motion may then be written as

$$u_t + \mathscr{L}u - 2\Omega nv - mnuv/a = -\frac{m}{a}(p/\rho_0)_\lambda + F^\lambda \tag{2.3}$$

and

$$v_t + \mathscr{L}v + 2\Omega nu + mnuu/a = -\frac{1}{a}(p/\rho_0)_\varphi + F^\varphi. \tag{2.4}$$

The hydrostatic relation is

$$\rho g = -p_z \tag{2.5}$$

and the continuity equation is

$$w_z + \frac{m}{a}\left[u_\lambda + (v/m)_\varphi\right] = 0. \tag{2.6}$$

There are two conservation equations,

$$T_t + \mathscr{L}T = Q \tag{2.7}$$

$$S_t + \mathscr{L}S = \sigma. \tag{2.8}$$

The effect of compression on the temperature is not included. This effect is relatively small and does not significantly alter the computation of density gradients in the horizontal plane, which determine the velocity field. The equation of state is based on an equation of the form

$$\rho = F(T, S, p). \tag{2.9}$$

A convenient algebraic expression for (2.9) is given by Eckart [6]. The effect of pressure in (2.9) may be taken into account with a high degree of accuracy by substituting $-\rho_0 gz$ for p. The terms F^λ, F^φ, Q, and σ present the effects of turbulent viscosity and diffusion. Let

$$\Delta\mu = m^2\mu_{\lambda\lambda} + m(\mu_\varphi/m)_\varphi. \tag{2.10}$$

Then

$$F^\lambda = A_v u_{zz} + \frac{A_M}{a^2}\{\Delta u + (1 - m^2n^2)u - 2nm^2v_\lambda\} \tag{2.11}$$

$$F^\varphi = A_v v_{zz} + \frac{A_M}{a^2}\{\Delta v + (1 - m^2n^2)v + 2nm^2u_\lambda\} \tag{2.12}$$

$$Q = \frac{A_v}{\delta}T_{zz} + \frac{A_H}{a^2}\Delta T \tag{2.13}$$

$$\sigma = \frac{A_v}{\delta}S_{zz} + \frac{A_H}{a^2}\Delta S. \tag{2.14}$$

The formulation of the F^φ and F^λ in the nonisotropic case, where mixing in the vertical differs from that in the horizontal, has been worked out by Saint-Guilly [17]. The formulation of mixing of momentum given by Bryan and Cox [3] is incorrect, although the error is only significant in polar latitudes.

In nature vertical mixing has a complex dependence on the density stratification, which is still very poorly understood. In the present model the effects of stratification are taken into account in a very simple manner which avoids

specification of extra parameters. In the model vertical mixing is uniform for all stable cases, and infinite in the unstable case. Let ρ'' be the density which a parcel of water would have if the *in situ* pressure is reduced to surface pressure. The delta in (2.13) and (2.14) is then given by

$$\delta = \begin{cases} 1, & (\rho'')_z < 0, \\ 0, & (\rho'')_z > 0. \end{cases} \tag{2.15}$$

Boundary conditions on velocity, temperature, and salinity at the lateral walls are

$$u, v, T_n, S_n = 0, \tag{2.16}$$

where $(\ )_n$ indicates a local derivative with respect to the coordinate normal to the wall. At the upper boundary,

$$\left.\begin{aligned} w &= 0 \\ \rho_0 A_v (u_z, v_z) &= \tau^\lambda, \tau^\varphi \end{aligned}\right\} z = 0, \tag{2.17}$$

where τ^λ and τ^φ are the zonal and meridional components of the surface stress, respectively. ρ_0 is the density of sea water at surface pressure and standard temperature and salinity.

In the case of temperature and salinity two boundary conditions are possible. Either the flux of heat and salinity may be specified, or the temperature and salinity fields themselves may be specified at the surface.

Setting $w = 0$ at the surface is called the "rigid-lid" approximation. The kinematic effects of small displacements of the upper surface are not taken into account. As outlined in the introduction this feature permits a much more efficient calculation, since it filters out the very high-speed surface gravitational-inertial waves.

At the lower boundary the very small effects of geothermal heat flow are neglected,

$$(T_z, S_z) = 0, \quad z = -H \tag{2.18}$$

$$w(-H) = -\frac{u(-H)}{a} m H_\lambda - \frac{v(-H)}{a} H_\varphi \tag{2.19}$$

and

$$\rho_0 A_v (u_z, v_z) = \tau_B^\lambda, \tau_B^\varphi. \tag{2.20}$$

The particular law used to calculate the bottom stress is not specified here. Several possibilities present themselves, of which Ekman theory is the simplest. Geostrophic drag laws, which have been developed by Gill [8] and others might also have advantages.

Elimination of Pressure

The formulation of the finite difference equations requires the elimination of pressure. Integrating the continuity equation with respect to z,

$$w(0) - w(-H) = -\frac{m}{a}\left[\left(\int_{-H}^{0} u\, dz\right)_\lambda + \left(\int_{-H}^{0} \frac{v}{m}\, dz\right)_\varphi\right] + \frac{u}{a}(-H) m H_\lambda + \frac{v}{a}(-H)\, H_\varphi. \tag{2.21}$$

At the surface the rigid lid requires that

$$w(0) = 0. \tag{2.22}$$

Combining (2.19), (2.21), and (2.22) it is possible to define a stream function such that

$$\begin{aligned} m\psi_\lambda &= a \int_{-H}^{0} \rho_0 v\, dz \\ \psi_\varphi &= -a \int_{-H}^{0} \rho_0 u\, dz. \end{aligned} \tag{2.23}$$

Making use of the hydrostatic relation

$$p(z) = p_s + g \int_z^0 \rho\, dz, \tag{2.24}$$

where p_s is the surface pressure.

To obtain a prediction equation for the transport stream function (2.3) and (2.4) are both integrated with respect to z and multiplied by $a\rho_0/mH$ and $a\rho_0/H$, respectively,

$$-(\psi_\varphi/Hm)_t = -(p_s)_\lambda + 2\Omega n \psi_\lambda/H + \frac{FU}{m} \tag{2.25}$$

$$m(\psi_\lambda/H)_t = -(p_s)_\varphi + 2\Omega n \psi_\varphi/H + FV, \tag{2.26}$$

where

$$FU = \frac{-a\rho_0}{H} \int_{-H}^{0} \left[\mathscr{L} u - mnuv/a - F^\lambda + \frac{gm}{a\rho_0} \int_z^0 \rho_\lambda\, dz'\right] dz \tag{2.27}$$

and

$$FV = \frac{-a\rho_0}{H} \int_{-H}^{0} \left[\mathscr{L} v + mnu^2/a - F^\varphi + \frac{g}{a\rho_0} \int_z^0 \rho_\varphi\, dz'\right] dz.$$

The surface pressure may be eliminated by cross-differentiating (2.25) and (2.26). The result is

$$(m\psi_\lambda/H)_{\lambda t} + (\psi_\varphi/Hm)_{\varphi t} = (FV)_\lambda - (FU/m)_\varphi - \psi_\lambda(2\Omega n/H)_\varphi + \psi_\varphi(2\Omega n/H)_\lambda. \tag{2.28}$$

Let the vertical average over the whole water column be indicated by an overbar,

$$\bar{(\ )} = \frac{1}{H}\int_{-H}^{0}(\ )\,dz \tag{2.29}$$

and the deviation from a vertical average by $\hat{(\ )}$. Thus the velocity components may be expressed as

$$(u, v) = (\bar{u}, \bar{v}) + (\hat{u}, \hat{v}). \tag{2.30}$$

The $\bar{u}$, $\bar{v}$ components may be predicted from (2.23) and (2.28). To predict $\hat{u}$, $\hat{v}$ we make use of (2.3) and (2.4) with the right-hand side of (2.24) substituted for the pressure term. The surface pressure, p_s, is temporarily set to zero:

$$u'_t + \mathscr{L}u - 2\Omega nv - mnuv/a = \frac{-mg}{\rho_0 a}\left(\int_z^0 \rho\,dz\right)_\lambda + F^\lambda \tag{2.31}$$

$$v'_t + \mathscr{L}v + 2\Omega nu + mnuu/a = \frac{-g}{\rho_0 a}\left(\int_z^0 \rho\,dz\right)_\varphi + F^\varphi. \tag{2.32}$$

u' and v' differ from u and v due to the neglect of that part of the pressure gradient force which depends on the surface pressure. To determine $\hat{u}$ and $\hat{v}$ we set

$$(\hat{u}, \hat{v}) = (u' - \bar{u}', v' - \bar{v}'). \tag{2.33}$$

In the determination of $\hat{u}$ and $\hat{v}$ the error due to the neglect of surface pressure in u' and v' is of no consequence, since that error is independent of z and is therefore eliminated by subtracting out $\bar{u}'$ and $\bar{v}'$.

III. BOUNDARY CONDITIONS ON THE TRANSPORT STREAM FUNCTION

In the simple case of a closed basin with no islands the boundary condition on (2.28) is simply that;

$$\psi = 0 \text{ (side boundaries)}. \tag{3.1}$$

The World Ocean with its many islands is a multiply connected region. At the shores of each island the boundary condition is

$$\psi = \mu_r, \quad r = 1, 2, 3, ..., R, \tag{3.2}$$

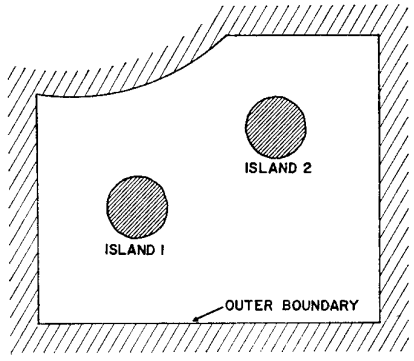

FIG. 1. A closed ocean basin with two islands.

where r is the index of the islands. In general μ is a function of time. The method for computing μ_r is based on that used by Kamenkovitch [9] in a study of the Antarctic circumpolar current.

Let $\mathbf{v}$ be the horizontal velocity vector and

$$(\mathbf{v})_t = -\nabla(p/\rho_0) + \mathbf{G}. \tag{3.3}$$

∇ is the horizontal grad operator and $\mathbf{G}$ is another horizontal vector representing the remaining terms in the equations of motion. The integrated form of (3.3), corresponding to (2.25) and (2.26), is

$$\mathbf{k} \times \nabla\psi_t = -\int_{-H}^{0}(\nabla p/\rho_0 - \mathbf{G})\,dz. \tag{3.4}$$

$\mathbf{k}$ is a unit vector normal to the horizontal plane. Dividing (3.4) by H and taking the curl of (3.4), we obtain

$$\nabla \times (\mathbf{k}/H \times \nabla\psi_t) = -\nabla \times \frac{1}{H}\int_{-H}^{0}(\nabla p/\rho_0 - \mathbf{G})\,dz. \tag{3.5}$$

Consider the closed basin with islands shown in Fig. 1. Let the transport stream function be represented by

$$\psi = \psi_0 + \sum_{r=1}^{R}\mu_r\psi_r. \tag{3.6}$$

In (3.6) only ψ_0 and μ_r are functions of time. The ψ_r fields satisfy the quation

$$\nabla \times (\mathbf{k}/H \times \nabla\psi_r) = 0 \tag{3.7}$$

with the boundary condition that

$$\begin{aligned} \psi_r &= 1 \quad \text{(perimeter of island } r\text{)} \\ \psi_r &= 0 \quad \text{(all other islands)}. \end{aligned} \tag{3.8}$$

Making use of the expression (3.6), the centered difference form of the local time derivative of the transport stream function is

$$\psi_t = \left[\psi_0^{l+1} + \sum_{r=1}^{R} \mu_r^{l+1} \psi_r - \psi^{l-1} \right] \Big/ 2\,\Delta t, \tag{3.9}$$

where the superscript l denotes the time level.

To calculate ψ_0 at each time level we make use of (3.5), (3.7), and (3.9),

$$\nabla \times (\mathbf{k}/H \times \nabla \psi_0^{l+1}) = \nabla \times (\mathbf{k}/H \times \nabla \psi^{l-1}) - 2\,\Delta t \left[\nabla \times \frac{1}{H} \int_{-H}^{0} (\nabla p/\rho_0 - \mathbf{G})\, dz \right] \tag{3.10}$$

with the boundary condition that

$$\psi = 0 \quad \text{(all boundaries)}. \tag{3.11}$$

To determine μ_r ($r = 1, 2, 3, ..., R$) we make use of a line integral of (3.4) along a path around each island. Let $\mathbf{s}$ represent a unit vector in the direction of the path of the line integral:

$$\oint \mathbf{s} \left[\mathbf{k}/H \times \nabla \sum_{r=1}^{R} \mu_r^{l+1} \psi_r \right] dS = -\oint \mathbf{s} \left\{ \mathbf{k}/H \times \nabla(\psi_0^{l+1} - \psi^{l-1}) - \frac{2\,\Delta t}{H} \int_{-H}^{0} [\nabla(p/\rho_0) - \mathbf{G}]\, dz \right\} dS. \tag{3.12}$$

R equations of the form of (3.12) for the paths around each island form a series of linear equations to determine μ_r^{l+1}, $r = 1, 2, 3, ..., R$. Note that the surface pressure can be eliminated from the right-hand side of (3.12). For a closed path

$$\oint \mathbf{s} \left[\frac{1}{H} \int_{-H}^{0} \nabla p_s\, dz \right] dS = 0, \tag{3.13}$$

where p_s is the surface pressure. Therefore, making use of (2.24),

$$\oint \mathbf{s} \left[\frac{1}{H} \int_{-H}^{0} \nabla p\, dz \right] dS = \oint \mathbf{s} \frac{g}{H} \left[\int_{-H}^{0} \left(\nabla \int_{z}^{0} \rho\, dz' \right) dz \right] dS. \tag{3.14}$$

IV. GENERAL METHOD OF FINITE DIFFERENCING

In constructing the finite differencing scheme we wish to ensure that certain integral constraints will be maintained. In particular, it is desirable to construct the finite difference equations so that momentum, energy, and the variance of temperature and salinity will be conserved in the absence of dissipative effects. The advantage of this approach was first pointed out by Arakawa [1]. Arakawa showed that, if integral constraints on energy are maintained, the computation will be free of the troublesome "nonlinear" instability originally pointed out by Phillips [15]. A consistent formulation of the energetic properties is also extremely important in carrying out long-term numerical integrations for an oceanographic model. Such a formulation will avoid systematic errors which will accumulate with time.

To give an example, let us consider the following equations for a scalar field q,

$$q_t + \nabla \cdot \mathbf{v} q = 0 \tag{4.1}$$

$$\nabla \cdot \mathbf{v} = 0, \tag{4.2}$$

where $\mathbf{v}$ is a velocity vector. Let $\mathbf{n}$ be the normal vector to the outer boundary of the total volume. The condition that the normal component of velocity vanish along the entire exterior boundary is given as

$$\mathbf{n} \cdot \mathbf{v} = 0. \tag{4.3}$$

Let the total volume under consideration be divided into η subvolumes or cells. The volume of each cell will be denoted as α_η. The average of q over each cell will be denoted as Q_η. Integrating (4.1) over each cell,

$$\alpha_\eta \frac{d}{dt} Q_n = -\oint q \mathbf{v} \cdot \mathbf{n}\, dS. \tag{4.4}$$

In this case $\mathbf{n}$ is a unit vector normal to the cell boundary. Our finite difference formulation will be based on (4.4) rather than the original differential equation (4.1).

Let each cell be bounded by B neighboring cells designated by the index b. In a regular rectangular array the total number of surrounding cells would be six, but it could be more or less, depending on the geometry. Let A_b be the area of each interface and V_b the normal velocity. Then (4.4) may be approximated by

$$\alpha_\eta \frac{d}{dt} Q_n = -\sum_{b=1}^{B} q_b V_b A_b, \tag{4.5}$$

where q_b is the value of q on the interface b. The corresponding continuity equation for the cell is

$$\sum_{b=1}^{B} V_b A_b = 0. \tag{4.6}$$

This approach in formulating finite difference equations is similar to that discussed by Noh [14].

The integral properties of a finite difference are particularly important in making a numerical integration with respect to time over a long period. Let

$$I_1 = \sum_{\eta=1}^{N} Q_\eta \alpha_\eta \tag{4.7}$$

$$I_2 = \sum_{\eta=1}^{N} Q_\eta^2 \alpha_\eta, \tag{4.8}$$

where N is the total number of cells in the entire volume, I_1 is the finite difference expression for the volume integral of q, and I_2 the volume integral of q^2. Summing (4.5) over all cells, we obtain

$$\frac{dI_1}{dt} = -\sum_{\eta=1}^{N} \sum_{b=1}^{B} q_b V_b A_b \tag{4.9}$$

$$\frac{dI_2}{dt} = -2 \sum_{\eta=1}^{N} \sum_{b=1}^{B} q_b Q_\eta V_b A_b. \tag{4.10}$$

It can be seen that $dI_1/dt = 0$, since the various terms on the right-hand side occur as pairs along all interior interfaces. The contribution on adjacent interfaces are equal and of opposite sign, cancelling each other when a sum is taken over the entire volume. Repeating the arguments given in [2], we see that in general the left-hand side of (4.10) does not vanish. It can be made to vanish, however, if we use an appropriate interpolation formula for the interface value of q_b,

$$q_b = (Q_\eta + Q_b)/2. \tag{4.11}$$

Here Q_b is the average value of q in the cell adjacent to the interface. Substituting (4.11) in (4.10),

$$\frac{dI_2}{dt} = -\sum_{\eta=1}^{N} \left[Q_\eta^2 \sum_{b=1}^{B} V_b A_b + \sum_{b=1}^{B} Q_\eta Q_b V_b A_b \right]. \tag{4.12}$$

Applying the continuity relation (4.6) we see that the first term on the right is zero. The second term on the right is made up of pairs of equal and opposite terms on interfaces. It vanishes due to the same cancelling effect that was discussed in connection with (4.9).

This simple example will indicate the motivation for the approach in designing the finite difference equations in the next section. The present method is a generalization of the ideas of Arakawa [1] which allows the arrangement of cells to be chosen in any manner that is convenient for the problem at hand.

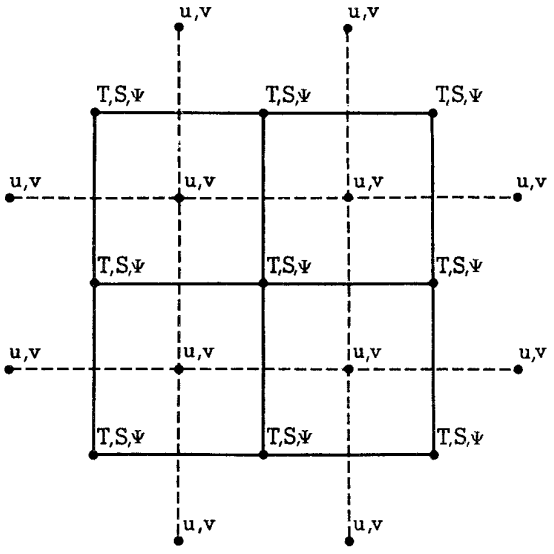

FIG. 2. The arrangement of variables in the horizontal plane for a grid with equal spacing in both directions.

V. ARRANGEMENT OF VARIABLES

Cells with the index i', j', and k' are placed so that they are centered on points given by the coordinates $\lambda_{i'}$, $\varphi_{j'}$, $z_{k'}$, where

$$\lambda_{i'} = \sum_{i=1}^{i'} \Delta_i \tag{5.1}$$

$$\varphi_0 - \varphi_{j'} = \sum_{j=1}^{j'} \Delta_j \tag{5.2}$$

$$z_{k'} = -\sum_{k=1}^{k'} \Delta_k. \tag{5.3}$$

The two horizontal components of velocity are averaged over cells centered on grid points given by integer indices, while temperature, salinity, and the stream function are centered on grid points, specified by $i' + \frac{1}{2}$, $j' + \frac{1}{2}$, and k'. In this case

$$\lambda_{i'+1/2} = \lambda_{i'} + \tfrac{1}{2}\Delta_{i'+1} \tag{5.4}$$

$$\varphi_{j'+1/2} = \varphi_{j'} - \tfrac{1}{2}\Delta_{j'+1}. \tag{5.5}$$

The arrangement of the variables in the horizontal plane is shown in Fig. 2. The pattern is similar to that used by Leith [10]. The motivation for choosing this arrangement is to obtain as close meshing of the variables as possible,

TABLE I

The Pattern of Variables[a]

	i	j	k
u, v	1	1	1
T, S	$\frac{1}{2}$	$\frac{1}{2}$	1
$w_{u,v}$	1	1	$\frac{1}{2}$
$w_{T,S}$	$\frac{1}{2}$	$\frac{1}{2}$	$\frac{1}{2}$

[a] An entry of 1 or 1/2 indicates whether a variable is located at an integer of half value of the index.

yet still to define both velocity components at the same time level and at the same point. The advantage of defining u and v at the same point will be discussed in the next section.

The vertical velocity must be calculated separately for the velocity points and for the salinity and temperature points. The vertical velocity points are located at the top and bottom interface of the cells and have the index $k' + \frac{1}{2}$, where

$$z_{k'+1/2} = z_{k'} - \tfrac{1}{2}\Delta_{k'+1/2}.$$

The arrangement of the variables is summarized in Table I.

VI. FINITE DIFFERENCE EQUATIONS

Using the "box method" we first write down the finite difference formulation of the momentum equation for the u' component given by (2.31). The dimensions of the cell are shown in Fig. 3a. The volume of the cell is given as

$$\alpha_1 = a^2\Delta_{i+1/2}\Delta_{j+1/2}\Delta_{k+1/2}/m_j, \tag{6.1}$$

where

$$\Delta_{i+1/2} = (\Delta_i + \Delta_{i+1})/2$$
$$\Delta_{j+1/2} = (\Delta_j + \Delta_{j+1})/2$$
$$\Delta_k = (\Delta_{k-1/2} + \Delta_{k+1/2})/2.$$

The finite difference equation is

$$\begin{aligned}\alpha_1[(u'^{l+1} - u^{l-1})/2\,\Delta t - \Omega n(v'^{l+1} + v^{l-1})] \\ = C_k - \frac{ag}{\rho_0}\Delta_{k+1/2}\Delta_{j+1/2}[\Delta_k(\rho_{i+1/2} - \rho_{i-1/2})|_{k=1} \\ + \sum_{q=2}^{k}(\rho_{i+1/2} - \rho_{i-1/2})_{q-1/2}\Delta_q,\end{aligned} \tag{6.2}$$

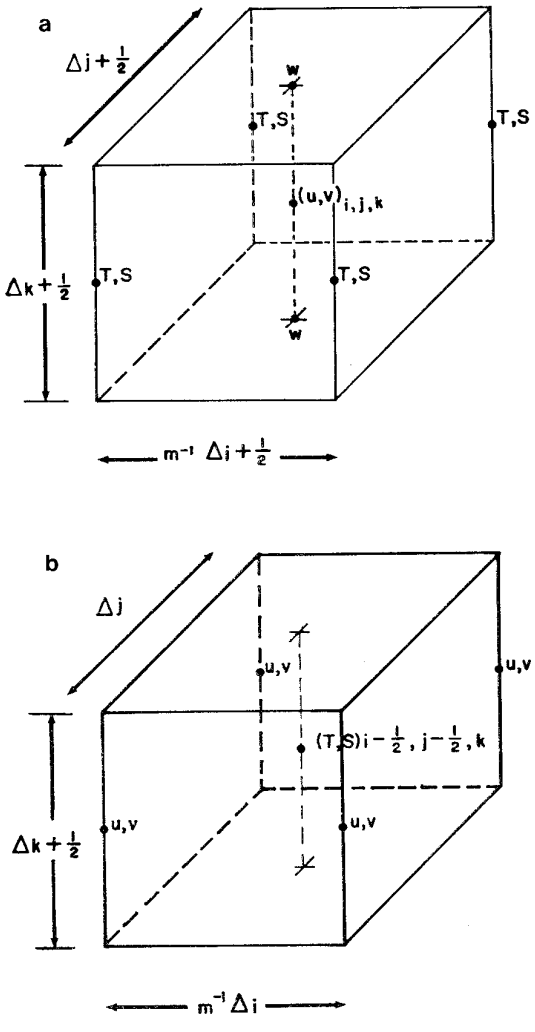

FIG. 3. (a) The finite difference cell-centered on the points at which the horizontal velocity is calculated. (b) The finite difference cell-centered on the temperature and salinity points.

where q is a dummy index for k. In (6.2) all indices are understood to be i, j, k, l, except as otherwise specified. Certain undefined variables occur in (6.2). For example, the density points are not defined on integer j-points. These points are understood to be simple averages of adjacent points where they are defined:

$$\rho_{j+1/2} + \rho_{j-1/2} = 2\rho_j$$
$$\rho_k + \rho_{k+1} = 2\rho_{k+1/2}.$$

The advection of momentum and the viscous terms are contained in C_k,

$$C_k = -\sum_{b=1}^{6} V_b A_b u_b + \alpha_1 uvmn/a + m^{-1}a^2 A_v(\Delta_{j+1/2}\Delta_{i+1/2})[(u_{k-1} - u_k)/\Delta_k - (u_k - u_{k+1})/\Delta_{k+1}]^{l-1} + A_M\{m\Delta_{j+1/2}\Delta_{k+1/2}[(u_{i+1} - u_i)/\Delta_{i+1} - (u_i - u_{i-1})/\Delta_i] + \Delta_{i+1/2}\Delta_{k+1/2}[(u_{j-1} - u_j)/m\Delta_j - (u_j - u_{j+1})/m\Delta_{j+1}] + \alpha_1(1 - n^2m^2)u/a^2 - 2nm\Delta_{j+1/2}\Delta_{k+1/2}(v_{i+1/2} - v_{i-1/2})\}^{l-1}. \tag{6.3}$$

Note that the viscous terms are lagged one time step behind the remaining terms on the right-hand side of (6.2). This means that the difference scheme is centered with respect to time for the pressure term and nonlinear terms, but forward time steps with an interval of 2 Δt are taken with respect to the viscous term. This arrangement is based on a discussion of the numerical stability of similar time-dependent problems given by Richtmyer [16].

The layout of variables in the horizontal plane of the numerical grid allows the Coriolis terms in (6.2) to be approximated by an average between the $l + 1$ and $l - 1$ time step. This arrangement is widely used in numerical models of the atmosphere in the Soviet Union [13]. It amounts to an implicit treatment of the Coriolis terms and allows a time step longer than the inertial period, if all other stability criteria are satisfied. This is particularly advantageous for a coarse grid with a mesh size of greater than 4° of latitude and longitude. A coarse grid of this type might be useful in ocean circulation calculations to save computation during the first period of adjustment. More detailed solutions are then obtained by interpolating the initial solutions to a finer grid.

The details of the nonlinear terms in (6.3) are shown below. Again all indices are understood to be i, j, k, l unless otherwise specified:

$$V_1A_1u_1 = \Delta_{k+1/2}\Delta_{j+1/2}u_{i+1/2} \times [a\hat{u}_{i+1/2} - (\psi_{i+1/2,j-1/2} - \psi_{i+1/2,j+1/2})/(H_1\Delta_{j+1/2})] \tag{6.4}$$

$$V_2A_2u_2 = -\Delta_{k+1/2}\Delta_{j+1/2}u_{i-1/2} \times [a\hat{u}_{i-1/2} - (\psi_{i-1/2,j-1/2} - \psi_{i-1/2,j+1/2})/(H_2\Delta_{j+1/2})] \tag{6.5}$$

$$V_3A_3u_3 = \Delta_{k+1/2}\Delta_{i+1/2}u_{j-1/2} \times \left[a\left(\frac{\hat{v}}{m}\right)_{j-1/2} + (\psi_{i+1/2,j-1/2} - \psi_{i-1/2,j-1/2})/(H_3\Delta_{i+1/2})\right] \tag{6.6}$$

$$V_4A_4u_4 = -\Delta_{k+1/2}\Delta_{i+1/2}u_{j+1/2} \times \left[a\left(\frac{\hat{v}}{m}\right)_{j+1/2} + (\psi_{i+1/2,j+1/2} - \psi_{i-1/2,j+1/2})/(H_4\Delta_{i+1/2})\right] \tag{6.7}$$

$$V_5A_5u_5 = \alpha_1 u_{k-1/2}w_{k-1/2}/\Delta_{k+1/2} \tag{6.8}$$

$$V_6A_6u_6 = -\alpha_1 u_{k+1/2}w_{k+1/2}/\Delta_{k+1/2}. \tag{6.9}$$

In (6.4)–(6.7) the terms $\hat{u}$ and $\hat{v}$ are defined as

$$(\hat{u}, \hat{v})_k = (u, v)_k - \frac{1}{H}\sum_{q=1}^{KM}(u_q, v_q)\Delta_{q+1/2}$$

and the depth values H_1, H_2, H_3, and H_4 are defined as

$$H_1 = \text{maximum of } (H_{i,j} \text{ or } H_{i+1,j}) \tag{6.10}$$

$$H_2 = \text{maximum of } (H_{i,j} \text{ or } H_{i-1,j}) \tag{6.11}$$

$$H_3 = \text{maximum of } (H_{i,j} \text{ or } H_{i,j-1}) \tag{6.12}$$

$$H_4 = \text{maximum of } (H_{i,j} \text{ or } H_{i,j+1}). \tag{6.13}$$

Separate diagnostic relations formed from the continuity equations are required to calculate the vertical velocity at u, v points and T, S points. For the calculation of

$$\frac{\alpha_1}{\Delta_{k+1/2}}(w_{k-1/2} - w_{k+1/2}) = -\sum_{b=1}^{4} V_bA_b \tag{6.14}$$

the terms V_1, V_2, V_3, and V_4 are given in brackets in (6.4)–(6.7).

The predictive equations for T, S are considerably simpler than the momentum equations. The cell that forms the basis of the "box" method is shown in Fig. 3b. The velocity points are in the same plane as the T, S points, but are located at the corners of the cell. The volume of the cell is given by

$$\alpha_2 = a^2\Delta_{i+1}\Delta_{j+1}\Delta_{k+1/2}/m_{j+1/2}. \tag{6.15}$$

In what follows all indices will be understood to be $i + \frac{1}{2}$, $j + \frac{1}{2}$, k, unless otherwise specified. The superscript l will also be understood. Only the predictive equation for T will be set down. The equation for S is identical to the prediction equation for T:

$$\begin{aligned}
&\alpha_2(T^{l+1} - T^{l-1})/2\,\Delta t \\
&\quad = -\sum_{b=1}^{6} V_b A_b T_b + A_v \frac{\alpha_2}{\Delta_{k+1/2}}[(T_{k-1} - T_k)/\Delta_k \\
&\qquad - (T_k - T_{k+1})/\Delta_{k+1}]^{l-1} \\
&\qquad + A_H a\{m\Delta_{j+1}\Delta_{k+1/2}[(T_{i+3/2} - T_{i+1/2})/\Delta_{i+3/2} \\
&\qquad - (T_{i+1/2} - T_{i-1/2})/\Delta_{i+1/2}] \\
&\qquad + \Delta_{i+1}\Delta_{k+1/2}[(T_{j-1/2} - T_{j+1/2})/m\Delta_{j+1/2} \\
&\qquad - (T_{j+1/2} - T_{j+3/2})/m\Delta_{j+3/2}]\}^{l-1}. \qquad (6.16)
\end{aligned}$$

The details of the advective term are given below,

$$A_1V_1T_1 = \frac{a}{2}\Delta_{k+1/2}T_{i+1}(u_{j+1}\Delta_{j+3/2} + u_j\Delta_{j+1/2})_{i+1} \qquad (6.17)$$

$$A_2V_2T_2 = \frac{-a}{2}\Delta_{k+1/2}T_i(u_{j+1}\Delta_{j+3/2} + u_j\Delta_{j+1/2})_i \qquad (6.18)$$

$$A_3V_3T_3 = \frac{a}{2m_j}\Delta_{k+1/2}T_j(v_{i+1}\Delta_{i+3/2} + v_i\Delta_{i+1/2})_j \qquad (6.19)$$

$$A_4V_4T_4 = \frac{-a}{2m_{j+1}}\Delta_{k+1/2}T_{j+1}(v_{i+1}\Delta_{i+3/2} + v_i\Delta_{i+1/2})_{j+1} \qquad (6.20)$$

$$A_5V_5T_5 = \frac{\alpha_2}{\Delta_{k+1/2}}T_{k-1/2}w_{k-1/2} \qquad (6.21)$$

$$A_6V_6T_6 = \frac{-\alpha_2}{\Delta_{k+1/2}}T_{k+1/2}w_{k+1/2}. \qquad (6.22)$$

To compute W corresponding to the $i + \frac{1}{2}, j + \frac{1}{2}$ points an equation similar to (6.14) is used with V_bA_b ($b = 1, 2, 3, 4$) given in (6.17)–(6.20) above.

At each time step preliminary values of T^{l+1} and S^{l+1} are predicted on the basis of (6.16) and a corresponding equation for salinity. Then the Eckart formula given by (2.9) in Section 2 is used to compute ρ^{l+1}. The entire water column is then tested for static stability. Let ρ'' be the density referred to surface pressure, corresponding to the *in situ* temperature and salinity. If

$$(\rho'')_k^{l+1} > (\rho'')_{k+1}^{l+1} \qquad (6.23)$$

for any value of k, the information is stored. After the entire water column is examined, T^{l+1} and S^{l+1} are reset so that the temperature and salinity are uniform over any group of adjacent layers for which (6.23) is satisfied,

$$(T'_k, T'_{k+1}, ..., T'_{k+N}) = \frac{\sum_{k'=k}^{k+N} T_{k'}\Delta_{k'+1/2}}{\sum_{k'=k}^{k+N}\Delta_{k'+1/2}}, \qquad (6.24)$$

where $k \cdots k + N$ are the indices of the adjacent unstable layers. The adjustment given by (6.24) corresponds to infinite mixing in the unstable part of the water column. A similar adjustment is done for salinity. When this has been carried out the entire column is scanned again to see if (6.23) is still satisfied at any point. If any instability is indicated, the entire process is repeated as many times as is necessary.

The relationship between the velocity components and the transport stream function is given by

$$a\sum_{k=1}^{K}\rho_0 u\Delta_{k+1/2} = -(\psi_{j-1/2} - \psi_{j+1/2})_i/\Delta_{j+1/2} \qquad (6.25)$$

$$a\sum_{k=1}^{K}\rho_0\left(\frac{v}{m}\right)\Delta_{k+1/2} = (\psi_{i+1/2} - \psi_{i-1/2})_{j+1/2}/\Delta_{i+1/2}. \qquad (6.26)$$

The vertically averaged velocity components will be written as $\bar{u}$ and $\bar{v}$. The components $\bar{u}$ and $\bar{v}$ may be obtained from the transport stream function by multiplying the right-hand side of (6.25) and (6.26) by $(\rho_0 aH)^{-1}$ and $(\rho_0 aH)^{-1}m$, respectively.

A predictive equation for the transport stream function completes the system. All variables have the subscript $i + \frac{1}{2}, j + \frac{1}{2}$ unless otherwise specified:

$$\begin{aligned}
&\Delta_{i+1}\Delta_{j+1}L(\psi^{l+1} - \psi^{l-1})/2\,\Delta t \\
&\quad = -\frac{1}{2}\left[\Delta_{i+1/2}\left(\frac{FU_{i,j}}{m_j} - \frac{FU_{i,j+1}}{m_{j+1}}\right)\right. \\
&\qquad \left. + \Delta_{i+3/2}\left(\frac{FU_{i+1,j}}{m_j} - \frac{FU_{i+1,j+1}}{m_{j+1}}\right)\right] \\
&\qquad + \frac{1}{2}[\Delta_{j+1/2}(FV_{i+1,j} - FV_{i,j}) \\
&\qquad + \Delta_{j+3/2}(FV_{i+1,j+1} - FV_{i,j+1})] \qquad (6.27) \\
&\qquad - \Omega\left\{\Delta_{i+1/2}\left[n_j\left(\frac{\bar{v}}{m}\right)_{i,j} - n_{j+1}\left(\frac{\bar{v}}{m}\right)_{i,j+1}\right]\right. \\
&\qquad + \Delta_{i+3/2}\left[n_j\left(\frac{\bar{v}}{m}\right)_{i+1,j} - n_{j+1}\left(\frac{\bar{v}}{m}\right)_{i+1,j+1}\right] \\
&\qquad + \Delta_{j+1/2}[n_j(\bar{u}_{i+1,j} - \bar{u}_{i,j})] \\
&\qquad \left. + \Delta_{j+3/2}[n_{j+1}(\bar{u}_{i+1,j+1} - \bar{u}_{i,j+1})]\right\}.
\end{aligned}$$

The operator L on the left-hand side of (6.27) is defined by (6.28):

$$
\begin{aligned}
L\psi = &\frac{m(\psi_{i+3/2} - \psi_{i+1/2})\Delta_{j+1}}{(H_{i+1,j}\Delta_{j+1/2} + H_{i+1,j+1}\Delta_{j+3/2})\Delta_{i+3/2}\Delta_{i+1}} \\
&- \frac{m(\psi_{i+1/2} - \psi_{i-1/2})\Delta_{j+1}}{(H_{i,j}\Delta_{j+1/2} + H_{i,j+1}\Delta_{j+3/2})\Delta_{i+1/2}\Delta_{i+1}} \\
&+ \frac{(\psi_{j-1/2} - \psi_{j+1/2})\Delta_{i+1}}{m_{j+1/2}(H_{i,j}\Delta_{i+1/2} + H_{i+1,j}\Delta_{i+3/2})\Delta_{j+1/2}\Delta_{j+1}} \\
&- \frac{(\psi_{j+1/2} - \psi_{j-3/2})\Delta_{i+1}}{m_{j+3/2}(H_{i,j+1}\Delta_{i+1/2} + H_{i+1,j+1}\Delta_{i+3/2})\Delta_{j+3/2}\Delta_{j+1}}.
\end{aligned} \tag{6.28}
$$

At each time step a second-order equation of the form $L\psi^{l+1} = M_{i+1/2,j+1/2}$ may be solved by relaxation, one of the few methods general enough to handle the complicated geometry of existing ocean basins. In the relaxation process the value of the transport stream function for the previous time step may be used as a first guess. This procedure greatly speeds up the convergence process.

The quantity FU in (6.27) is yet to be defined:

$$
\begin{aligned}
FU_{ij} = &\frac{a\rho_0}{H_{ij}} \sum_{k=1}^{K_{ij}} (\Delta_{k+1/2} C_k/\alpha_1) \\
&- \frac{g}{H_{ij}} \sum_{k=1}^{K_{ij}} \frac{m\Delta_{k+1/2}}{\Delta_{i+1/2}} \left\{ \Delta_k(\rho_{i+1/2} - \rho_{i-1/2})|_{k=1} \right. \\
&\left. + \sum_{q=2}^{k} \Delta_q(\rho_{i+1/2} - \rho_{i-1/2})_{q-1/2} \right\}.
\end{aligned} \tag{6.29}
$$

The expression for FV has an exactly parallel form. As before q corresponds to a dummy vertical index within the summation with respect to k.

It is now possible to summarize the numerical integration procedure. New values of temperature and salinity are predicted from equations of the form given in (6.16). Relation (6.2) and a corresponding equation for the v-component serve to predict $(u', v')^{l+1}$. These components are then used to find the new values of $(\hat{u}, \hat{v})^{l+1}$,

$$
(\hat{u}, \hat{v})^{l+1} = (u', v')^{l+1} - \frac{1}{H} \sum_{k=1}^{K} (u', v')^{l+1} \Delta_{k+1/2}. \tag{6.30}
$$

The predicted values of $(\bar{u}, \bar{v})$ may be obtained from (6.25) and (6.26) using the new value of the transport stream function.

Once new time levels for the predicted variables have been found, the diagnostic relations based on the continuity equation and the equation of state are used to find w and ρ for the new time level. Experience has shown [12] that repeated use of the leap-frog time differencing scheme may lead to a serious "split" between adjacent time levels. This is caused by the fact that centered differences artificially change the prediction equations from first to second order with respect to time. Following a suggestion made by Arakawa,[1] this difficulty is circumvented by periodically substituting a forward time step for the centered time step. This procedure is equivalent to throwing away one of the two solutions at regular intervals before the "split" becomes significant. A ratio of 23 leap-frog time steps to one forward time step is a typical value used in one rather extensive calculation.

VII. BOUNDARY CONDITIONS OF THE FINITE DIFFERENCE EQUATIONS

The basic information on boundary conditions is the number of cells stacked downward from the surface at each T, S point given by the indices, $i + \frac{1}{2}$, $j + \frac{1}{2}$. Let the number of cells be given as $K_{i+1/2,j+1/2}$, then

$$
H_{i+1/2,j+1/2} = \sum_{k=1}^{K_{i+1/2,j+1/2}} \Delta k. \tag{7.1}
$$

The number of cells at velocity points is then given by

$$
\begin{aligned}
K_{ij} = &\text{ Minimum of} \\
&(K_{i+1/2,j+1/2}, K_{i-1/2,j+1/2}, K_{i-1/2,j-1/2}, K_{i+1/2,j-1/2}).
\end{aligned} \tag{7.2}
$$

The depth at i, j may then be calculated according to a formula corresponding to (7.1). The boundary condition on velocity is very simple,

$$
(u, v)_{i,j} = 0, \quad k > K_{i,j}, \tag{7.3}
$$

and in the case of the transport stream function,

$$
\psi_{i+1/2,j+1/2} = \text{const}, \quad K_{i+1/2,j+1/2} = 0 \tag{7.4}
$$

$$
\psi_{i+1/2,j} - \psi_{i-1/2,j} = 0, \quad K_{ij} = 0 \tag{7.5}
$$

$$
\psi_{i,j-1/2} - \psi_{i,j+1/2} = 0, \quad K_{ij} = 0. \tag{7.6}
$$

The constant in (7.4) has a different value for the shores of the mainland and each island. The procedure for computing these values is given in Section 3.

In the case of temperature and salinity the boundary condition must be set for each point adjacent to a wall. Due to the irregular bottom topography the boundary condition may change from one level to the next for any single point in the horizontal plane. First a test is made. If

$$
k > K_{i+1/2+A,j+1/2+B} \tag{7.7}
$$

[1] Personal communication.

then

$$T_{i+1/2+A,j+1/2+B,k} = T_{i+1/2,j+1/2,k}, \tag{7.8}$$

where

$$(A, B) = (1, 0), (-1, 0), (0, 1), (0, -1). \tag{7.9}$$

The test given by (7.7) indicates whether k exceeds the maximum number of levels at any adjacent temperature and salinity point. This indicates the existence of an adjacent wall. The exact computational procedure used to set the boundary condition according to (7.7)–(7.9) will naturally depend on the computing equipment used. In some cases it may be optimum to test during the course of the computations. In other cases it may be more efficient to store the results of tests carried out in an initial inspection in the form of a table. The table would then be used to set the boundary conditions.

VIII. FINITE DIFFERENCE FORMULATION OF ISLANDS

The formulation in the case of islands is straightforward, if somewhat cumbersome. The method follows the outline given for the continuous equations in Section 3. If R is the number of islands it is necessary to include $R + 1$ separate fields for the stream function:

$$\psi^l = \psi_0{}^l + \sum_{r=1}^{R} \mu_r{}^l \psi_r. \tag{8.1}$$

Only ψ_0 is a function of time, the remaining fields, ψ_r, are kept fixed and stored in the permanent memory of the machine. It is only necessary to recompute an amplitude μ_r for each island, at each time step.

Let $\mathbf{G}$ be some horizontal vector such that

$$\mathbf{G} = \mathbf{i}G^x + \mathbf{j}G^y. \tag{8.2}$$

We define the numerical equivalent of a line integral in terms of an operator B,

$$\begin{aligned} B\mathbf{G} = &\sum_{i=I}^{I+\Delta I} [G^x_{i,J} - G^x_{i,J+\Delta J}] \frac{\Delta_{i+1/2}}{m} \\ &+ \sum_{j=J}^{J+\Delta J} [G^y_{I+\Delta I,j} - G^y_{I,j}] \Delta_{j+1/2}. \end{aligned} \tag{8.3}$$

The line integral is taken counterclockwise in the i, j plane. The integral given in (8.3) is a simple rectangular path. In some cases it may not be possible to construct simple rectangular paths around islands, because of other nearby islands or continental boundaries. In such cases it would be necessary to construct a more complicated path around the perimeter of several adjoining rectangles of various shapes.

Corresponding to (3.6) it is possible to define the vertically averaged flow vector as

$$\bar{\mathbf{v}}^l = \bar{\mathbf{v}}_0 + \sum_{r=1}^{R} \mu_r{}^l \bar{\mathbf{v}}_r, \tag{8.4}$$

where

$$\begin{aligned} \bar{\mathbf{v}} = (aH)^{-1} [&-\mathbf{i}(\psi_{i,j-1/2} - \psi_{i,j+1/2})/\Delta_{j+1/2} \\ &+ \mathbf{j}m(\psi_{i+1/2,j} - \psi_{i-1/2,j})/\Delta_{i+1/2}]. \end{aligned} \tag{8.5}$$

Using the operator given in (8.3) to denote the line integral around a closed path, it is possible to write the finite difference equivalent of 3.12 as

$$\begin{aligned} &B[1 + 2\Omega n\, \Delta t \mathbf{k} \times (\quad)] \left(\bar{\mathbf{v}}_0^{l+1} + \sum_{r=1}^{R} \mu_r^{l+1} \bar{\mathbf{v}}_r \right) \\ &\quad = B[1 - 2\Omega n\, \Delta t \mathbf{k} \times (\quad)] \bar{\mathbf{v}}^{l-1} + 2\, \Delta t B\, (\mathbf{i}FU + \mathbf{i}FV)^l. \end{aligned} \tag{8.6}$$

The terms FU and FV in (8.6) have previously been defined in (6.29) of the previous section. It is possible to write R equations like (8.6) for closed paths around each island. Since the right-hand side of (8.6) is known, these R relations constitute a set of linear equations sufficient to find μ_r. The matrix of coefficients on the left of (8.6) can be determined, then inverted and stored in memory at the beginning of the computation, since they do not vary with time. Once the left-hand side of (8.6) is calculated at each time step, μ_r^{+1} can then be computed by a simple matrix multiplication.

IX. COMPUTATIONS CARRIED OUT WITH THE METHOD

To illustrate how the method could be applied, two examples will be sketched briefly. Detailed results will be given elsewhere. The layout of the grid for the first computation carried out by M. D. Cox is shown in Fig. 4. The area covers the Indian Ocean, extending from the Asian continent down to 18° S. On the west it is bounded by Africa, and on the east by the meridian at 102° E and the Malayan Peninsula. The first stage of the calculation was carried out with a 4° mesh and six levels in the vertical direction. Temperature, salinity, and wind stress fields taken from climatic atlases are specified at the surface as a function of season of the year. In the first stage of the calculation it is possible to take a time step of 12 h, each time step requiring 10 s to compute on a *UNIVAC* 1108

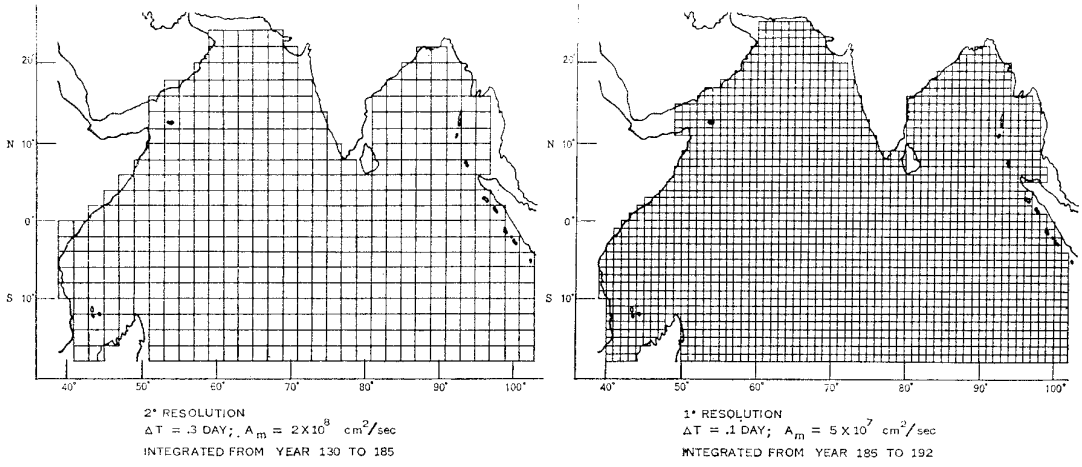

FIG. 4. Numerical grid used for calculation of the seasonal changes in circulation of the Indian Ocean. (Left) 2° resolution and (right) 1° resolution.

computer. Only a few fields are stored permanently in the 65K rapid access memory of the machine. Most of the fields are kept on the magnetic drums and cycled through the memory when needed. Shifts from magnetic drums to memory take place while the computation is in progress, so that no extra time is required for the transfer process.

Experience indicates that it is advantageous to start with a large value of A_M and decrease this value as the grid is successively refined. The lateral diffusion coefficient, A_H, is kept at a low value throughout the computation. The motivation for this procedure is that the density field adjusts itself very slowly, while the velocity field can adjust relatively rapidly to any change in the lateral friction coefficient. Each new stage of the computation must be started with a forward time step followed by centered time steps.

The layout of the grid in the second and third stages of the computation is shown in Fig. 4. The final mesh size is 1° of latitude and longitude. Along the open boundary the transport stream function is taken from charts of Sverdrup transport computed by Welander [20]. The temperature and salinity distributions in the vertical section, which encloses the area, were taken from hydrographic data supplied by the World Oceanographic Data Center *A*. Let $\hat{u}$ and $\hat{v}$ denote the deviation of the velocity components from the vertical mean. The total transport through the boundary is determined by the transport stream function, and the gradients normal to the boundary of $\hat{u}$ and $\hat{v}$ are set equal to zero. This condition allows the vertical profile of the inflow and outflow to adjust geostrophically to the density field specified at the boundary.

A second computation performed with the present model is part of a study of the thermohaline circulation of the southern hemisphere oceans. The final pattern of the mass transport stream function is shown in Fig. 5, based on an average taken over the final part of the run to remove the effect of persistent fluctuations. The basin includes spherical geometry and extends from the equator to 70°S with a gap in the meridional wall at about 60°. Cyclic boundary conditions are assumed in the gap, so that the flow coming in is exactly like that going out. The total flow through the gap must be computed according to the Kamenkovitch method outlined in Section III. The computation is carried out for a rotation rate one order of magnitude less than that of the earth. The ocean circulation is

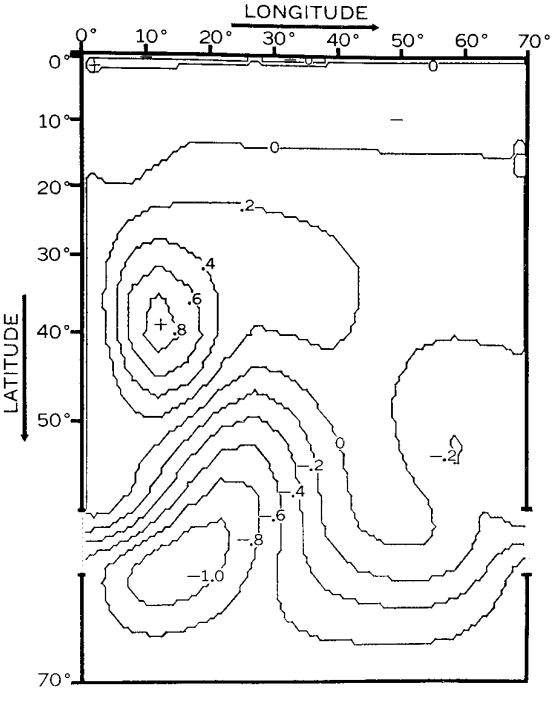

FIG. 5. The pattern of transport stream function obtained in a theoretical study of the Antarctic Circumpolar Current.

being driven by both a wind stress distribution and a density gradient imposed at the surface. Initially all density surfaces are flat and the fluid is at complete rest. The low rotation explains the unrealistic width of the western boundary current.

The computation is carried out for a flat bottom. A variable mesh width is used to provide extra resolution along all lateral boundaries. The smallest mesh interval near the wall is approximately 1°, while in the interior the grid points are spaced approximately 6° apart. There are eight levels in the vertical. A typical time step is 1/10 of a day, and the equilibrium solution in Fig. 5 is after 30 years of model time. This required a total of 200 h of machine time on the Univac 1108. To examine the realistic case with the correct rotation rate for the earth requires even more computation, since the time to reach equilibrium is longer, and the boundary currents are narrower and require more grid points for accurate resolution.

APPENDIX

In order to be sure that a universal scheme will be useful for studying the behavior of a hydrodynamic system over an extended period, careful checks should be made of the energy balance. The choice of numerical scheme given in this paper is largely motivated by energy considerations. Only an energy consistent scheme will avoid the special type of instability described by Phillips [15] without excessive damping of important features of the flow.

Let

$$K = \bar{K} + \hat{K}, \tag{A.1}$$

where

$$\bar{K} = \rho_0(\bar{u}^2 + \bar{v}^2)/2 \tag{A.2}$$

and

$$\hat{K} = \rho_0(\hat{u}^2 + \hat{v}^2)/2. \tag{A.3}$$

$\bar{K}$ may be considered the kinetic energy of the external mode, and $\hat{K}$ the kinetic energy of the internal mode. Let $\{\ \}$ designate the volume integral over a closed ocean basin. If we multiply the left-hand side of (2.28) by $m\psi/(a^2H\rho_0)$ and integrate over the entire volume,

$$\left\{\frac{\psi m}{a^2H\rho_0}[(m\psi_{\lambda t}/H)_\lambda + (\psi_{\varphi t}/Hm)_\varphi]\right\}$$
$$= \left\{\frac{m}{a^2H\rho_0}[(m\psi\psi_{\lambda t}/H)_\lambda + (\psi\psi_{\varphi t}/Hm)_\varphi]\right\} \tag{A.4}$$
$$- \frac{1}{2}\left\{\frac{m^2}{a^2}\psi^2_{\lambda t}/H^2\rho_0 + \frac{1}{a^2}\psi^2_{\varphi t}/H^2\rho_0\right\}.$$

The first term on the right vanishes with the boundary condition that $\psi = 0$ along the lateral boundaries. Therefore,

$$\{\bar{K}_t\} = -\left\{\frac{\psi m}{a^2H\rho_0}[(m\psi_{\lambda t}/H)_\lambda + (\psi_{\varphi t}/Hm)_\varphi]\right\}. \tag{A.5}$$

Multiplying the right-hand side of (2.28) by $-\psi m/(a^2H\rho_0)$ we obtain

$$\{\bar{K}_r\} = I_1 + I_2 + I_3 + I_4, \tag{A.6}$$

where,

$$I_1 = \left\{\frac{\psi m}{a^2H}\left[\left(\frac{a}{H}\int_{-H}^{0}\mathscr{L}v\,dz\right)_\lambda - \left(\frac{a}{Hm}\int_{-H}^{0}\mathscr{L}u\,dz\right)_\varphi\right]\right\} \tag{A.7}$$

$$I_2 = \left\{\frac{\psi m}{a^2H}\left[\left(\frac{mn}{H}\int_{-H}^{0}u^2\,dz\right)_\lambda + \left(\frac{n}{H}\int_{-H}^{0}uv\,dz\right)_\varphi\right]\right\} \tag{A.7a}$$

$$I_3 = \left\{\frac{-\psi m}{a^2H}\left[\left(\frac{a}{H}\int_{-H}^{0}F^\varphi dz\right)_\lambda - \left(\frac{a}{Hm}\int_{-H}^{0}F^\lambda dz\right)_\varphi\right]\right\} \tag{A.8}$$

$$I_4 = \left\{\frac{\psi m}{a^2H}\left[\left(\frac{1}{H}\int_{-H}^{0}(p - p_s)_\varphi\,dz\right)_\lambda - \left(\frac{1}{H}\int_{-H}^{0}(p - p_s)_\lambda\,dz\right)_\varphi\right]\right\}. \tag{A.9}$$

The complete expression for $p - p_s$ is given in (2.24).

In order to write down an expression for $\hat{K}_t$, (2.31) and (2.32) must be multiplied by $\rho_0\hat{u}$ and $\rho_0\hat{v}$, respectively. Integrating the sum of the results over the entire volume,

$$\{\hat{K}_t\} = I_5 + I_6 + I_7 + I_8 \tag{A.10}$$

$$I_5 = -\{\rho_0\hat{u}\mathscr{L}u + \rho_0\hat{v}\mathscr{L}v\} \tag{A.11}$$

$$I_6 = \left\{\frac{\rho_0 mn}{a}(\hat{u}uv - \hat{v}uu)\right\} \tag{A.11a}$$

$$I_7 = \{\rho_0\hat{u}F^\lambda + \rho_0\hat{v}F^\varphi\} \tag{A.12}$$

$$I_8 = -\left\{\frac{\hat{u}m}{a}(p - p_s)_\lambda + \frac{\hat{v}}{a}(p - p_s)_\varphi\right\}. \tag{A.13}$$

To demonstrate the energetic consistency of our model we wish to show that: (a) the nonlinear terms in the difference equations have no net effect on the total amount of kinetic energy; and (b) the exchange terms between potential and kinetic energy are correctly accounted for. The requirement (a) is satisfied if

$$I_1 + I_5 = 0 \tag{A.14}$$

$$I_2 + I_6 = 0. \tag{A.14a}$$

The requirement (b) is equivalent to

$$I_4 + I_8 = -\{g\rho w\},$$

or

$$= -\left\{ g w_z \int_{-z}^{0} \rho \, dz \right\}. \tag{A.15}$$

To prove that (A.14) and (A.15) hold for the present numerical scheme involves rather complicated algebraic manipulation. To simplify the derivations we will use a notation and approach similar to that of Lilly [11].

Let

$$2\overline{\eta}^{\lambda} = \eta_{i+1/2} + \eta_{i-1/2} \tag{A.16}$$

$$\delta_\lambda \eta = \eta_{i+1/2} - \eta_{i-1/2}. \tag{A.17}$$

We have the following rules:

$$\eta \delta_\lambda \beta + \overline{\beta \delta_\lambda \eta}^{\lambda} = \delta_\lambda(\overline{\eta}^{\lambda} \beta) \tag{A.18}$$

and

$$\overline{\overline{\eta}^{\lambda} \beta}^{\lambda} - \eta \overline{\beta}^{\lambda} = \tfrac{1}{4} \delta_\lambda (\beta \delta_\lambda \eta). \tag{A.19}$$

(A.18) and (A.19) may be easily verified by simply substituting (A.16) and (A.17). It is obvious that (A.16)–(A.19) hold in the same way, if φ is substituted for λ.

Substituting ζ^{φ} for β in (A.18) and making use of (A.19) we obtain

$$\eta \delta_\lambda \overline{\zeta}^{\varphi} + \overline{\zeta \overline{\delta_\lambda \eta}^{\varphi}}^{\varphi\lambda} = \delta_\lambda(\overline{\eta}^{\lambda} \overline{\zeta}^{\varphi}) + \tfrac{1}{4} \delta_\varphi (\overline{\zeta \delta_\varphi \delta_\lambda \eta}^{\varphi})^{\lambda}. \tag{A.20}$$

As in the case of (A.18) and (A.19) the rule given by (A.20) is also valid if φ and λ are exchanged at all points in the equation.

An expression for I_1 may be obtained by multiplying (6.27) by ψ and summing over all half integer points. Note that it is only necessary to multiply by $a\psi$ rather than $a\psi m/H$, since the factor m/H cancels out in the volume integral:

$$I_1 = -\sum_{i+1/2} \sum_{j+1/2} a\psi \left[\delta_\varphi \overline{\left(\overline{\mathscr{L}u}^{\varphi} \Delta_{i+1/2} \right)}^{\lambda} - \delta_\lambda (\overline{\mathscr{L}v}^{\varphi} \Delta_{j+1/2}) \right]. \tag{A.21}$$

The overbar without a superscript indicates a vertical average, while the overbars with superscripts are the two point horizontal averages defined by (A.16):

$$\begin{aligned} I_1 = -a \sum_{i+1/2} \sum_{j+1/2} \Bigg[& \overline{\left(\frac{-\overline{\delta_\varphi \psi}^{\lambda}}{\Delta_{j+1/2}} \overline{\mathscr{L}u} + \frac{\overline{m \delta_\lambda \psi}^{\varphi}}{\Delta_{i+1/2}} \overline{\mathscr{L}v} \right) \Delta_{i+1/2} \Delta_{j+1/2} m^{-1}}^{\varphi\lambda} \\ & + \delta_\varphi \left(\overline{\psi}^{\varphi} \overline{\frac{\mathscr{L}u}{m} \Delta_{i+1/2}}^{\lambda} \right) - \delta_\lambda (\overline{\psi}^{\lambda} \overline{\mathscr{L}v \, \Delta_{j+1/2}}^{\varphi}) \\ & + \frac{1}{4} \delta_\lambda \left(\delta_\lambda \delta_\varphi \psi \cdot \overline{\frac{\mathscr{L}u}{m} \Delta_{i+1/2}} \right) - \frac{1}{4} \delta_\varphi (\delta_\lambda \delta_\varphi \psi \cdot \overline{\mathscr{L}v} \, \Delta_{j+1/2}) \Bigg]. \end{aligned} \tag{A.22}$$

The boundary conditions on the transport stream function given in Section 7 are such that the last four terms of (A.22) vanish. We also note that (6.25) and (6.26) give

$$(\overline{u}, \overline{v}) = \frac{1}{a \rho_0 H} \left(-\frac{\overline{\delta_\varphi \psi}^{\lambda}}{\Delta_{j+1/2}}, m \frac{\overline{\delta_\lambda \psi}^{\varphi}}{\Delta_{i+1/2}} \right). \tag{A.23}$$

Substituting (A.23)–(A.22) and rejecting the terms which vanish on integration,

$$I_1 = -\sum_{i+1/2} \sum_{j+1/2} a^2 \overline{[\rho_0 H (\overline{u}\,\overline{\mathscr{L}u} + \overline{v}\,\overline{\mathscr{L}v}) \, \Delta_{i+1/2} \Delta_{j+1/2} m^{-1}]}^{\varphi\lambda}. \tag{A.24}$$

It is now possible to combine I_1 and I_5 as

$$I_1 + I_5 = -\sum_{i+1/2} \sum_{j+1/2} \sum_{k} a^2 \rho_0 \overline{[(\overline{u} + \hat{u}) \, \mathscr{L}u + (\overline{v} + \hat{v}) \, \mathscr{L}v] \, \Delta_{i+1/2} \Delta_{j+1/2} \Delta_{k+1/2} m^{-1}}^{\varphi\lambda}, \tag{A.25}$$

where we have made use of the relation

$$H \overline{u}\,\overline{\mathscr{L}u} = \sum_{k} \overline{u} \mathscr{L}u \Delta_{k+1/2}. \tag{A.26}$$

From (6.3) it can be seen that (A.25) may be written as

$$\begin{aligned} I_1 + I_5 = -\sum_{i+1/2} \sum_{j+1/2} \sum_{k+1/2} a^2 \alpha_1^{-1} \rho_0 \Bigg[& (\overline{u} + \hat{u}) \sum_{b=1}^{6} m V_b A_b u_b \\ & + (\overline{v} + \hat{v}) \sum_{b=1}^{6} m V_b A_b v_b \Bigg] \Delta_{i+1/2} \Delta_{j+1/2} \Delta_{k+1/2} m^{-1}, \end{aligned} \tag{A.27}$$

where

$$\sum_{b=1}^{6} V_b A_b = 0 \tag{A.28}$$

is the local continuity equation for each cell. To demonstrate that $I_1 + I_5$ vanishes, it is only necessary to repeat the arguments given in Section 4. The nonlinear terms will not change the average kinetic energy of the entire volume if u_b and v_b are defined as the arithmetic average between adjacent cells. This completes the derivation of (A.14). To derive (A.14a) we follow the same procedure shown in (A.21)–(A.25), where I_2 replaces I_1 and I_6 replaces I_5. Since the demonstration is closely parallel to that for (A.14) we avoid writing out the detailed equations.

Next we investigate the pressure force terms. If we multiply (6.27) by ψ, the arguments of (A.21)–(A.24) may be repeated to show that

$$I_4 = -\sum_{i+1/2}\sum_{j+1/2}\sum_{k}\overline{\left[\frac{\bar{u}m}{a}\frac{\delta_\lambda\overline{(p-p_s)}^{\varphi}}{\Delta_{i+1/2}} + \frac{\bar{v}}{a}\frac{\delta_\varphi\overline{(p-p_s)}^{\lambda}}{\Delta_{j+1/2}}\right]\Delta_{i+1/2}\Delta_{j+1/2}\Delta_{k+1/2}m^{-1}}^{\varphi\lambda}. \tag{A.29}$$

Let (6.2) be multiplied by $\hat{u}$ and an equivalent equation for the v'-component be multiplied by $\hat{v}$, combining the results and integrating:

$$I_8 = -\sum_{i+1/2}\sum_{j+1/2}\sum_{k}\overline{\left[\frac{\hat{u}m}{a}\frac{\delta_\lambda\overline{(p-p_s)}^{\varphi}}{\Delta_{i+1/2}} + \frac{\hat{v}}{a}\frac{\delta_\varphi\overline{(p-p_s)}^{\lambda}}{\Delta_{j+1/2}}\right]\Delta_{i+1/2}\Delta_{j+1/2}\Delta_{k+1/2}m^{-1}}^{\varphi\lambda}. \tag{A.30}$$

The sum $I_4 + I_8$ is then a similar expression with $\hat{u}$ and $\hat{v}$ replaced by the total components u and v, respectively.

Next we make use of (A.20). The result is that

$$I_4 + I_8 = \sum_{i+1/2}\sum_{j+1/2}\sum_{k}(p-p_s)\,\Delta_{k+1/2}\left[\delta_\lambda\overline{(u\Delta_{j+1/2})}^{\varphi} + \delta_\varphi\overline{\left(\frac{v}{m}\Delta_{i+1/2}\right)}^{\lambda}\right]. \tag{A.31}$$

The continuity equation at $i + \frac{1}{2}$, $j + \frac{1}{2}$ points is

$$am^{-1}\Delta_{i+1}\Delta_{j+1}\frac{\delta_z w}{\Delta_{k+1/2}} = -\delta_\lambda\overline{(u\,\Delta_{j+1/2})}^{\varphi} - \delta_\varphi\overline{\frac{v}{m}\Delta_{i+1/2}}^{\lambda}. \tag{A.32}$$

Substituting (A.32) in (A.31),

$$I_4 + I_8 = -\sum_{i+1/2}\sum_{j+1/2}\sum_{k} a^2[(p-p_s)\,\delta_z w]\,\Delta_{i+1}\Delta_{j+1}m^{-1}. \tag{A.33}$$

The expression (A.33) is the equivalent of (A.15) for the continuous case and completes the derivation.

ACKNOWLEDGMENTS

Much of the credit for the final form of the numerical model is due to Mr. M. D. Cox. Mr. Cox designed the program to test the numerical model and contributed many ideas to overcome the difficulties which arose as the work progressed. The author is very grateful to Dr. Adrian Gill for pointing out the work of V. M. Kamenkovitch for calculating the transport around islands and to Mr. Sol Hellerman for writing a program to test the island formulation in the numerical model. The assistance of Miss Martha Jackson in preparing the figures, and Mrs. Dolores Drake and Mrs. Christine Morgan in typing the manuscript is also appreciated.

REFERENCES

1. A. Arakawa, *J. Comput. Phys.* **1,** 119 (1966).
2. K. Bryan, *Mon. Wea. Rev.* **94,** 39 (1966).
3. K. Bryan and M. D. Cox, *Tellus* **19,** 54 (1967).
4. K. Bryan and M. D. Cox, *J. Atmos. Sci.* **25,** 945 (1968).
5. W. P. Crowley, *J. Comput. Phys.* **3,** 111 (1968).
6. C. Eckart, *Amer. J. Sci.* **256,** 225 (1958).
7. J. E. Fromm, *Los Alamos Rep.* **2910** (1963).
8. A. E. Gill, *Q. J. R. Met. Soc.* **94,** 586 (1968).
9. V. M. Kamenkovitch, *Trudy Inst. Okeanol.* [Akad. Nauk SSSR] **56,** 241 (1962).
10. C. E. Leith, "Methods in Computational Physics" (B. Alder and S. Fernbach, Eds.), Vol. 4, Academic Press, New York, 1965.
11. D. K. Lilly, *J. Atmos. Sci.* **21,** 83 (1964).
12. D. K. Lilly, *Mon. Wea. Rev.* **93,** 11 (1965).
13. G. I. Marchuk, *Dokl. Akad. Nauk SSSR* **155,** 1062 (1964).

14. W. F. Noh, ''Methods in Computational Physics'' (B. Alder and S. Fernbach, Eds.), Vol. 3. Academic Press, New York, 1965.
15. N. A. Phillips, Contribution to ''The Atmosphere and the Sea in Motion,'' p. 501, Rockefeller Press, New York, 1959.
16. R. D. Richtmyer, ''Difference Methods for Initial Value Problems,'' Wiley (Interscience), New York, 1957.
17. B. Saint-Guilly, *Ann. L'Inst. Ocean. (Paris)* **33,** 1 (1956).
18. A. S. Sarkisyan, *Izv. Akad. Nauk SSSR, Ser. Geofiz.* **6,** 554 (1955).
19. A. S. Sarkisyan, *Okeanologia* **11:3,** 393 (1962).
20. P. Welander, Contribution to ''The Atmosphere and the Sea in Motion,'' p. 95, Rockefeller Press, New York, 1959.